Astron. Astrophys. 95, 349–361 (1981)

ASTRONOMY
AND
ASTROPHYSICS

Merging of Galaxies in an Expanding Universe

N. Roos

Sterrewacht, Huygens Laboratorium, P.O. Box 9513, 2300 RA Leiden, The Netherlands

Received May 30, 1979; accepted July 30, 1980

Summary. Expanding universe models containing 400 equal mass galaxies are numerically simulated and the effects of galaxy collisions are specifically included. Initially the galaxies are distributed at random with low velocity dispersion relative to the Hubble flow. The merging rate is insensitive to galactic parameters since most mergers occur between galaxies in bound orbits. The final fraction of merged galaxies is found to be approximately 10–40% in both the open and closed universe models. Both galaxy clustering and the evolution of the galaxy mass function seem consistent with a simple infall model. The clustering properties of merged systems in the simulations are in agreement with those observed for bright elliptical galaxies. The clustering properties of lenticular galaxies suggest that they form a class intermediate between ellipticals and spirals. The mass function evolution is investigated further by Monte Carlo simulations on a randomly distributed system of galaxies where the merging probability of a pair of galaxies is chosen to be proportional to their combined mass. Such a merging probability, consistent with the results of the expanding universe simulations, gives a mass spectrum that approaches a self-similar form identical to the Press and Schechter mass function in the case of random initial fluctuations. It is also consistent with the infall model. It is proposed to identify the bulge to disk ratio parameter with the ratio of the infallen mass to the original mass. It is shown that the observed frequencies of different galaxy types as a function of mass and local galaxy density can be modelled in this way.

Key words: cosmology – merging – galaxy types

1. Introduction

Galaxies can interact strongly and this fact must necessarily be incorporated into most investigations of their properties. This paper presents the results of numerical studies concerning the effects of galaxy collisions on the formation, evolution and clustering of galaxies. Our aim is to elucidate and extend current models of galaxy formation that invoke galaxy mergers in an expanding universe.

The general technique adopted here and in recent work (Jones and Efstathiou, 1979, hereafter JE and Aarseth and Fall, 1980, hereafter AF) is to utilize studies of individual galaxy-galaxy collisions (Van Albada and Van Gorkom, 1977; White, 1978; Roos and Norman, 1979, Paper I) and incorporate the relevant collisional cross-sections into standard expanding universe calculations (Miyoshi and Kihara, 1975; Aarseth et al., 1979; Turner et al., 1979; Gott et al., 1980).

The suggestion brought forward by Toomre and Toomre (1972, see also Toomre, 1977) that elliptical galaxies would be the result of mergers between galaxies of comparable size has gained considerable support recently in numerical N-body simulations which showed that (i) the final frequency and clustering properties of merged particles in a study of the evolution of individual groups and clusters (Paper I) and in expanding universe simulations (JE, AF) are very similar to those of bright elliptical galaxies, (ii) the characteristic angular momentum of merged particles in the cosmological experiments agrees with the low rotation velocities found in elliptical galaxies, (iii) merger products of spherically symmetric galaxies of comparable mass tend to have a Hubble density profile (White, 1979; Villumsen, 1979). The principal thrust of this paper is to investigate in detail the clustering properties and mass function evolution of the merged systems and to try to make the natural extension of the merger model of ellipticals to explain the origin of other morphological types as the result of mergers between galaxies of unequal mass.

The next section deals with the numerical experiments. In Sect. 3 the merging rate, clustering properties and mass function of the particles in the simulations are discussed. It is proposed that the latter two properties can be interpreted using a simple infall model. In Sect. 4 observed frequencies and clustering properties of elliptical and SO galaxies are compared with those of merged galaxies in the simulations. We consider briefly the evidence that galaxy mass is indeed correlated with local galaxy density as predicted by the infall model. A model is presented for the evolution of a realistic initial mass function during the epoch of cluster formation. Its implications for the origin of different galaxy types are discussed in Sect. 6.

2. Numerical Experiments

Before discussing the detailed calculations and results of the present work it seems useful to make a comparison with other recent studies. The merging criteria in our calculations are only slightly different from those used by JE and AF. Mass-loss and loss of orbital energy during collisions are additional effects considered here. The total orbital and internal energy of a merging pair was not strictly conserved. This is not important since in this paper we are not primarily interested in the structural properties of the merged systems. In fact the mass-radius relations found by AF, who do conserve total orbital and internal energy, is very similar to the one we have used. In our $\Omega=1$ models most of the de-

celeration of the universe is modelled by an extra force component due to some uniformly distributed hot constituent.

2.1. The Code

The numerical N-body code is basically the same as the one used by Aarseth et al. (1979, hereafter AGT) so we will merely mention the differences here. Collision effects were included. No particles were reflected at the boundary R of the exanding sphere. However, at the end of the run the density in the outer shell between $0.9\ R$ and R was not significantly lower than the overall density. In the case of a critical universe an extra radial force component decelerating the expansion was added, mimicking the effect of a universal component. This force is given at time t by $F(t)=-\frac{1}{2}H^2(t)c\boldsymbol{r}$, where c is the ratio of the density of the dynamically hot component to the critical density, $H(t)$ is the Hubble parameter and $|r|$ is the distance to the centre of the expanding sphere.

2.2. Initial Conditions

Initially all 400 galaxies have equal mass M_g. Following AGT, their luminosity L_g is chosen to be that of a typical bright galaxy, which means $L_g \simeq L^* \simeq 3\,10^{10}\,L_\odot$ (Turner and Gott, 1976; Schechter, 1976). The mass-to-light ratio of the galaxies and the clusters that are formed is then $100\ M_\odot/L_\odot\ (M_g/3\,10^{12}\,M_\odot)$. Adopting a luminosity density of $5\,10^7\,L_\odot\ \mathrm{Mpc}^{-3}$ the final number density of our galaxies should be $n_g \simeq 1.7\,10^{-3}\ \mathrm{Mpc}^{-3}$. The final value of the Hubble parameter in the simulations is $50\ \mathrm{km\ s^{-1}\ Mpc^{-1}}$. The initial radius of the expanding boundary sphere R_i is chosen to produce about the right amount of clustering in the final state as measured by the amplitude of the spatial covariance function.

The particles are placed at random inside the initial volume so that the density fluctuations follow a Poissonian distribution. The distribution of peculiar velocities is taken to be an isotropic Maxwellian with a dispersion of $50\ \mathrm{km\ s^{-1}}$, so that the ratio of kinetic energy in random motions to the kinetic energy in the expansion is initially much smaller than unity and the universe is cold as predicted by the standard big bang model. Although the initial velocity perturbations should be related to the density fluctuations in the galaxy distribution, the fluctuations in both the density and velocity distributions are small and therefore we neglect this effect. At the start of the simulations individual galaxies represent density fluctuations

$$(\delta\varrho/\varrho)_g=(1-c)\,(R_i/R_g)^3/N_i+c-1$$

where R_g is the galaxy radius, and N_i is the initial number of galaxies. The initial density contrast is $(\delta\varrho/\varrho)_g \sim 1$ in the $\Omega=1$ models and $\sim 10^0$–10^4 in the open models. In some models the sensitivity of the final state to changes in the initial small scale distribution was tested.

2.3. Collision Parameters

As in Paper I, the galaxy potential was taken to be proportional to $(r^2+\varepsilon^2)^{-1/2}$. In a collision, the softness parameter ε has a strong effect on the velocity v and separation p at closest approach. The inelasticity of a collision is determined by v and p and so one has to be careful in choosing ε. The collision velocity measured in the numerical calculations of Paper I is, for $p/R_1 \lesssim 1$, and $v_\infty \lesssim \sigma_g$, approximated by

$$v^2=8.8\,\sigma_g^2(1-0.4\,p/R_1)\left(\frac{1+M_2/M_1}{2}\right)+v_\infty^2, \tag{1}$$

where $M_1 \geqq M_2$, v_∞ is the relative velocity at infinity, σ_g the internal velocity dispersion of the galaxies (assumed to be equal for the two galaxies) and R_1 is the radius of the largest galaxy with mass M_1. The radius R_1 is defined as twice the half-mass radius and σ_g^2 is proportionality to GM_g/R_g; the constant of proportionality is determined by the structure of the galaxies, which is assumed not to change in collisions. For the galaxies used in the collision calculations we had $\sigma_g^2=0.72\,GM_g/R_g$. In the present calculations where galaxies are treated as softened pointmasses the collision velocity is

$$v^2=4\,GM_1\left(\frac{1+M_2/M_1}{2}\right)(p^2+\varepsilon^2)^{-1/2}+v_\infty^2.$$

The collision calculations in Paper I indicate that σ_g does not change much in collisions, and so $R_g \propto M_g$. We find

$$v^2=5.6\,\sigma_g^2 R_1\left(\frac{1+R_2/R_1}{2}\right)(p^2+\varepsilon^2)^{-1/2}+v_\infty^2 \tag{2}$$

In order to match (1) and (2) we need $\varepsilon/R_1=0.64$ in the case $p=0$. If $p=R_1$ we need $\varepsilon/R_1=0.3$. Most collisions occur between galaxies in bound orbits with small ellipticities more consistent with the value 0.6. In the simulations ε/R_1 ranged from 0.34 to 0.57. Although the velocities for the nearly head-on collisions will be overestimated with small ε/R_1, the loss of orbital energy is still large and generally the collision velocity was below v_{crit} at the second or third impact.

All collisions with $p>R_1$ were purely elastic. For the critical upper limit to the relative velocity between galaxies with mass M_1 and M_2 $(M_1 \geqq M_2)$ for mergers to still occur we have used

$$v_{\mathrm{crit}}(p)=3.2\,\sigma_g(1-0.3\,p/R_1)\left(\frac{1+M_2/M_1}{2}\right)^{1/4}$$

(see Paper I). Particles may also lose orbital energy and mass in non-merging collisions. The energy loss is then effectuated by decreasing their relative momentum instantaneously at closest approach. The loss of orbital kinetic energy E is prescribed by

$$\Delta E/E=12.25\left(\frac{\sigma_g}{v}\right)^4(1-0.8\,p/R_1)\,(1+M_2/M_1) \quad \text{for} \quad p<R_1$$

$$=0 \quad \text{for} \quad p>R_1$$

and the mass-loss by

$$\Delta M=6.1\left(\frac{\sigma_g}{v}\right)^2(1-0.8\,p/R_1)M_2 \quad \text{for} \quad v>v_{\mathrm{crit}}(p)$$

$$\Delta M=\tfrac{1}{2}M_2 \quad \text{for} \quad v<v_{\mathrm{crit}}(p).$$

This mass-loss can be regarded as an upper limit. Firstly, most collision calculations in Paper I were done for hyperbolic orbits while most mergers in the expanding universe simulations occur between galaxies in bound orbits. Secondly, the "lost" mass was defined as the mass ejected across a spherical surface radius $2R_g$ around the parent galaxy. Most of this mass is still bound to the galaxy but forms an extended low density halo which is dynamically unimportant. Experiments without mass-loss were also made. As described in Paper I, the mass that a galaxy should have lost in collisions is stored until it exceeds half the initial mass of the galaxies. A background particle is then created and sent away from the parent galaxy in a random direction at the escape velocity. In all experiments we have used $\varepsilon \propto R_g \propto M_g$ throughout a run.

Table 1. Results of numerical experiments

	N_f	$R_{i,f}$ Mpc	$H_{i,f}$ 100 km s^{-1} Mpc^{-1}	Ω_f	c	σ_f 100 km s^{-1}	M_g 10^{12} $M_\odot$	R_g Mpc	$v_{crit}(p=0)$ 100 km s^{-1}	ε/R_g	A_f	N_M/N_f
1	341	5.0 –35.5	9.2 -0.5	1	0.8	1.15	6	0.34	7.6	0.35	5	0.13
2	309	2.5	26.1			1.4					10	0.21
3	263	0.7	177.0			1.8					30	0.27
4	247	0.7	177.0			2.4		0.07	16.0	0.43	50	0.29
5	266	0.7	177.0			2.1		0.07	16.0	0.43	50	0.29
6	337	0.7	177.0		0.9	1.1	3	0.07	11.3	0.43	10	0.15
7	258	2.06–35	13.7 -0.5	0.1	0.0	1.5	3	0.17	7.6	0.35	15	0.29
8	166	38.3	17.4	0.15		1.6	6	0.07	16.0	0.57	25	0.33
9	232	48.0	19.41	0.08		1.8	6	0.07	16.0	0.57	30	0.28
10*a	218	48.0	19.41	0.08		1.5	6	0.07	16.0	0.57	30	0.33
b	238	48.0	19.41	0.08		1.4	6	0.34	7.6	0.57	30	0.31
c	260	48.0	19.41	0.08		2.1	6	0.01	44.5	0.57	40	0.24
11	176	1.64–10.5	-0.1	$\sim 10^2$		—					$\simeq 400$	0.41
12	326	2.59–51	-0.6	$\sim 2.10^{-2}$		—					$\simeq 4$	0.16

Column (1) gives the model number. Underlined numbers are standard models which means that the subsequent models until the next standard model have the same parameters unless specified otherwise. Column (2) gives the final number of galaxies ($N_i=400$) and column (3) the initial and final radius of the expanding boundary sphere. Columns (4)–(7) give the initial and final Hubble parameter, the final ratio of the density over the critical density Ω_f, the value of c and the final velocity dispersion of the galaxies resp. The galaxy mass and radius are given in columns (8) and (9), the critical velocity for head-on collisions between equal mass galaxies in (10) and ε/R_g in (11). The final amplitude of the covariance function A_f in column (12) was estimated from the typical excess number density of galaxies at a distance $0.8<r<1.2$ Mpc from a galaxy. Column (13) gives the final fraction of merged galaxies.

* Note: model 10a was run three times and 10b twice with different random numbers. The given quantities are averages over these runs

2.4. Results

A series of N-body numerical experiments was performed with the aim of testing the sensitivity of the final fraction of merged galaxies and the amplitude of the covariance function to various parameters. The details of each experiment are contained in Table 1.

Models 1–3 have different R_i/R_f, where subscript i denotes the initial state and subscript f the final state. The galaxies in model 4 have smaller size than in models 1–3. Models 5 and 6 were constructed to test the sensitivity to the small scale distribution of the particles. The separation for two neighbouring galaxies with initially zero orbital energy is $s=(2\Omega_i/N_i)^{1/3}R_i$. The galaxies in 5 have initial separation larger than 0.53 s. In model 6 the minimum separation was 0.67 s.

In model 8 and 10 the galaxies were constrained to undergo no mass-loss in collisions.

Models 9 and 10 have a lower final number density.

The initial galactic radius, R_g, was varied in models 10a, b, and c.

Models 11 and 12 are similar to 7 except that in 11 the initial density was $2\varrho_i$ (7), and $0.5\varrho_i$ (7) in model 12, where ϱ_i (7) is the initial density in model 7. These models were run for a same time interval as model 7 and can be regarded as regions of high and low density respectively in the model 7 universe. The excess density around a galaxy in these models was calculated with respect to the mean density in the model 7 universe.

The four principal results from Table 1 are:

(i) The evolution of the amplitude of the covariance function is consistent with standard models (Gott and Rees, 1975).

(ii) The amplitude of the covariance function is approximately proportional to the initial galactic mass.

(iii) From our simulations we estimate galaxy collapse times of $\sim 10^9$ yr for $\Omega<1$ and $\sim 10^8$ yr for $\Omega=1$.

(iv) The final fraction of merged galaxies (10–40%) is very insensitive to galactic parameters and to Ω_f. It is weakly correlated with the amplitude of the covariance function.

We shall now discuss the first three results. The final point will be discussed in the following section.

(i) We expect that $A_f \propto (1+z_{st})^\beta$ where z_{st} is the initial redshift, with $\beta=2$ in the linear regime and $\beta=3+\gamma$ thereafter, when the spatial covariance function $\xi(r)$ is described by a simple power law $\xi(r)=A(r/1\text{ Mpc})^\gamma$ and $(1+z_{st})<\Omega_f^{-1}$ (cf. AGT). In our simulations we find $\gamma\simeq -2$ consistent with previous work. We expect therefore that β varies from ~ 2 at early epochs to ~ 1 at late epochs (see also Sect. 3.1). From A_f and R_i/R_f in models 1, 2, and 4 we find $\langle\beta\rangle\sim 1.2$. A_f in model 3 is lower than expected because the initial separation between neighbours was comparable to ε. The value we find for $\langle\beta\rangle$ is somewhat lower than the value 1.6 used by AGT because merging reduces the number of particles on small scales resulting in a decrease of A_f. For example, AGT find $A_f\simeq 70$ when $z_{st}=17$ while we find $A_f\simeq 25$ in model 8 which has comparable parameters (M_g, z_{st}, and A_f; the index of the initial density fluctuation spectrum does not seem to affect A_f). This indicates that merging has reduced A_f by about a factor 3, and in the absence of merging we would expect $\langle\beta\rangle\simeq 1.2+\log 3=1.7$.

(ii) The mass dependence of A_f is most evident when we compare our results for the $\Omega=1$ universe with those of AGT. They

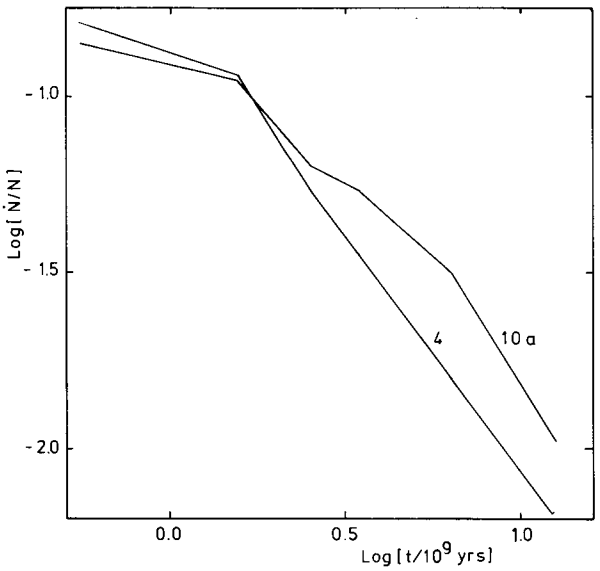

Fig. 1. Evolution of the merging rate in model 4 and 10a. N is the number of mergers per 10^9 yr

give $A_f \simeq 70$ for $z_{st}=9.9$ and $M_g = 5\,10^{13}$ $M_\odot$. Assuming $A_f \propto (1+z_{st})^{1.7}$ M_g and including a factor 1/3 for the effect of merging, we expect $A_f = 37$ in our model 4, in reasonable agreement with the experimental result. A plausible explanation for the relation between A_f and M_g found here is provided by the infall model of Gunn and Gott (1972). On the basis of this model it is expected that the infall rate onto a galaxy or cluster of galaxies is proportional to its total mass.

(iii) Galaxy collapse times can be estimated for $1+z_{st} > \Omega_f^{-1}$ by

$$T_c \simeq \pi H_0^{-1} \Omega_f^{-1/2} (1+z_{st})^{-1.5}.$$

Using $A_f (1+z_{st})^{1.7}$ we find from the results of model 10 that $1+z_{st} \simeq 40[M_g/6\,10^{12}\,M_\odot]^{-0.6}$ to obtain $A_f \sim 70$. This yields an estimate of the galaxy collapse time in the case of an open universe with $\Omega_f = 0.1$ of $T_c \simeq 10^9$ yr. In the $\Omega = 1$ universe we find $1+z_{st} \simeq 60\,[M_g/6\,10^{12}\,M_\odot]^{-0.6}$ and $T_c \simeq 10^8$ yr.

3. Properties of Merged Galaxies

3.1. The Total Number of Merged Galaxies and the Merging Rate

The total number of mergers in the simulations is remarkably insensitive to galactic parameters as well as to Ω_f. The reason is that most mergers occur between galaxies in bound pairs (cf. AF). The initial fraction of bound pairs is calculated by assuming that particles are distributed at random with number density n. Then the total fraction of galaxies having their nearest neighbour within radius r is $F(r) = 1 - \exp[-\frac{4}{3}\pi n r^3]$ (Chandrasekhar, 1943). The maximal initial separation for bound pairs, those with zero binding energy, is $s = 0.78\,\Omega_i n^{-1/3}$. Then $F(s) = 1 - \exp[-1.99\,\Omega_i^3]$ which is 86% if $\Omega_i = 1$. Even for an open universe with $\Omega_f \ll 1$, $\Omega_i \lesssim 1$, since

$$\Omega_i = (1 + (\Omega_f^{-1} - 1) R_i/R_f)^{-1}$$

and for $R_i/R_f \sim 23$ and $\Omega_f \sim 0.08$, $\Omega_i = \sim 0.67$ and $F(s) = 45\%$. Therefore, the number of initially bound pairs is very insensitive to Ω_f in our models. The galaxies in a bound pair will eventually merge unless the pair is disrupted in a cluster. From the simulations we see that about 60% of the galaxies merge with their nearest neighbour. The initial velocity dispersion of the galaxies is low and thus the ellipticity of the bound orbits is generally large. Therefore most collisions are almost head-on and the galaxies merge at first impact, forming systems with low characteristic angular momentum (JE, AF). The fraction of merged galaxies can be calculated from the total number of mergers $N_i - N$, where N is the current galaxy number. Assuming that the merging probability is independent of mass, it is not difficult to show that $N_M/N = 1 - N/N_i$, which is typically $\sim 40\%$ at the end of the simulations. The fraction of merged galaxies in the simulations is $\sim 30\%$ indicating that merged galaxies have a higher merging probability than other galaxies.

We now estimate the collision rate assuming that nearest neighbours fall together in the free fall time $(2\,GM_g/R_1^3)^{-1/2}$, where R_1 is the distance between nearest neighbours. This assumption seems justified when nearest neighbours are approaching each other, requiring $\sigma_p > R_1 H$. R_1 can be estimated using the correlation function which can be defined by

$$\xi(r) = \frac{n(r) - \bar{n}}{\bar{n}} = A\,(r/1\ \mathrm{Mpc})^{\gamma}.$$

Clearly $\xi(r)$ is the typical excess density relative to the mean density $\bar{n}$ at a distance r from a galaxy. The nearest neighbour distance R_1 is then

$$R_1 = \left(\frac{3+\gamma}{4\pi\bar{n}A}\right)^{\frac{3}{3+\gamma}}$$

and the collision rate per galaxy

$$C = \frac{1}{2}\left(\frac{2GM_g}{R_1}\right)^{1/2} \tag{3}$$

$$= \frac{1}{2}(2GM_g)^{1/2}\left(\frac{4\pi\bar{n}A}{3+\gamma}\right)^{\frac{3}{6+2\gamma}}$$

Substituting the parameters for model 10a at t_f ($\gamma = -2$) we find $R_1 = 5.6$ Mpc and $C = 0.09\ (10^{10}\ \mathrm{yr})^{-1}$. The final collision rate in model 10a averaged over the interval $10^{10} < t < 1.6\,10^{10}$ yr is $0.20 \pm 0.09\ (10^{10}\ \mathrm{yr})^{-1}$. In the next section we will see that the mean mass of colliding galaxies in model 10 is about 2.7 M_g which will increase our estimated C to $0.15\ (10^{10}\ \mathrm{yr})^{-1}$.

In Fig. 1 the evolution of the merging rate in models 10a and 4 is shown. The evolution of the merging rate cannot be described by (3) since $\sigma_p/(R_1 H) \simeq (GM_g/R_1^3)^{1/2} H^{-1} = CH^{-1} \lesssim 1$, at the end of the simulation, but $\sigma_p/(R_1 H) \ll 1$ at earlier epochs. The temporal behaviour of the merging rate is very similar to the increase of mass within a fixed distance D of a galaxy.

$$\frac{1}{M}\frac{dM}{dt} = 4\pi D \frac{d}{dt}[\bar{n}A].$$

Using a proper separation coordinate we have $A = A_f (R/R_f)^{\beta-\gamma}$, where β changes from ~ 2 at early epochs to ~ 1 at late epochs. Assuming $\gamma = -2$ we find

$$\frac{1}{M}\frac{dM}{dt} = 4\pi D \bar{n}_f A_f t^{\frac{2\beta-5}{3}} \quad \text{if} \quad \Omega = 1$$

$$= 4\pi D \bar{n}_f A_f t^{\beta-2} \quad \text{if} \quad \Omega < 1.$$

The merging rate at the end of the simulations drops slightly faster than t^{-1} probably because the merging efficiency K, defined by the ratio of the number of mergers over the number of collisions, decreases with t. The evolution of K in some models is given in

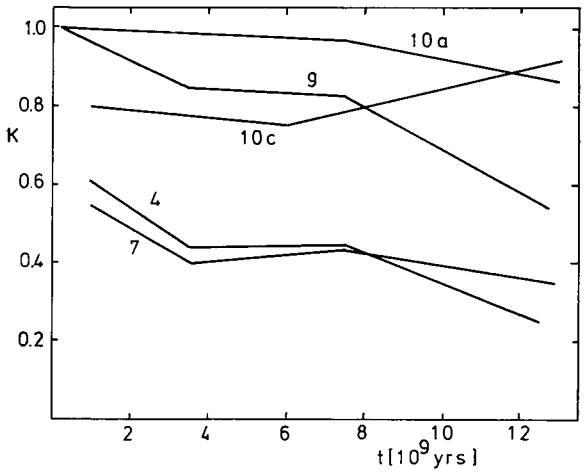

Fig. 2. Ratio of the number of mergers to the number of collisions as a function of time

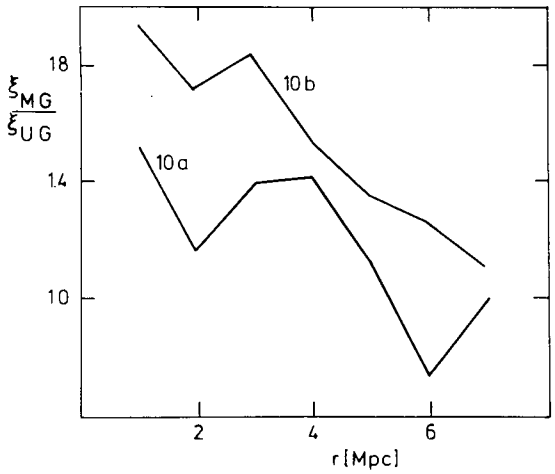

Fig. 3. Ratio of the correlation functions of merged (M) to unmerged (U) galaxies with other galaxies in model 10a and 10b at t_f

Fig. 2. In model 10 $K \lesssim 1$ even at large t, indicating that merging has strongly prevented the formation of virialised clusters with velocity dispersion larger than σ_g. In models 4 and 7, ε/R_g is smaller than in model 10 and it takes a few collisions before the galaxies merge, so that $K \simeq 0.4$. This will increase the covariance function on small scales by about a factor K^{-1} but will not affect the merging rate.

3.2. *Clustering Properties of Merged Galaxies*

The simulations show that on small scales the excess density of galaxies around merged galaxies ξ_{M_g} is higher than around unmerged galaxies ξ_{UG} (see Fig. 3). A similar phenomenon was found by Gott et al. (1979, hereafter GTA) who give results for an expanding universe in which two-third of the galaxies were given mass m and one-third mass $2m$. They found that on the scale of a typical interparticle distance R_1 (hereafter called the local scale) the covariance function of the more massive galaxies was about twice that of the covariance function of the less massive ones. On larger scales the two covariance functions become equal. These results are interpreted on the basis of the infall model of Gunn and Gott (1972). In this model the effect of the local density enhancement of a cluster mass m embedded in a homogeneous expanding universe is considered. They show that the infall rate of matter onto the cluster is proportional to m. In our simulations we deal with a discrete distribution of particles of comparable mass. We will show that, as long as virialised groups and clusters of particles do not form, the results of the simulations are consistent with an infall model in which the probability $P(m)$ that a merging pair has total mass m, is proportional to $m\phi(m)$, where $\phi(m)$ is the fraction of all pairs having total mass m. $P(m)$ can be written as

$$P(m)=\frac{\sum\limits_{m_i+m_j=m}(m_i+m_j)}{\sum\limits_{i,j}(m_i+m_j)} \tag{4}$$

where summations are over all possible pairs. Such a probability law is expected if all particles are distributed at random independent of their mass. In this case the probability that a close pair has mass m and separation lying between r and $r+dr$ can be written as $4\pi\bar{n}\phi(m)r^2dr$. The collapse time of a close pair is given by $t_c \simeq (Gm/r^3)^{-1/2}$ and the probability that a pair has mass m and collapse time in the interval $[t_c, t_c+dt_c]$ is $4\pi\bar{n}Gm\phi(m)t_c dt_c$. For a given collapse time, the probability that a collapsing or merging pair has total mass m is proportional to $m\phi(m)$.

In Fig. 4 we have plotted the function $N_p(m)/\phi(m)$ where $N_p m$ is the number of pairs with total mass m and separation less than R_1. Equation (4) seems to apply throughout the evolution of model 10b, while in 10a the experimental relation deviates from Eq. (4) with increasing time. The particles in model 10a are much smaller and collapsed groups or clusters are less easily destroyed by merging. The merging rate among small galaxies is depressed most strongly and the number of relatively low mass neighbours increases.

The distribution of masses for merging pairs should also obey (4) if merging prevents the formation of clusters. From (4) it follows that the parameter

$$T(m)=\frac{\sum\limits_{m_i+m_j<m}(m_i+m_j)+\frac{1}{2}\sum\limits_{m_i+m_j=m}(m_i+m_j)}{\sum\limits_{i,j}(m_i+m_j)} \tag{5}$$

determined each time a merger occurs between two galaxies of total mass m must be uniformly distributed on $[0, 1]$ with $\langle T\rangle=\frac{1}{2}$. This test was suggested by White (1980, private communication). Figure 5 shows $\langle T\rangle$ for mergers in different time intervals in models 10a, b, and c. The best agreement is found for the models with large galaxy radii. The mean value of all mergers $\langle T\rangle=0.52$ when $R_g=340$ kpc, and $\langle T\rangle=0.58$ when $R_g=10$ kpc. A further test of Eq. (4) is to count the number of mergers among galaxies of different type during a time interval in which the mass-function is assumed constant. When the merging probability is given by (4) it can be shown that

$$N_{UU}:N_{UM}:N_{MM}=1:(\langle m\rangle_M+1)f_M/f_U:\langle m\rangle_M(f_M/f_U)^2. \tag{6}$$

Here, N_{UM} is the number of mergers among merged and unmerged galaxies, $f_M$and f_U are the fractions of merged and unmerged galaxies, $\langle m\rangle_M$ is the average mass of the merged galaxies, and unmerged galaxies have unit mass (see Sect. 3.3). In Table 2 the relative numbers of mergers in models 10a, b, c are given with the prediction from (6). The last three columns give the time-

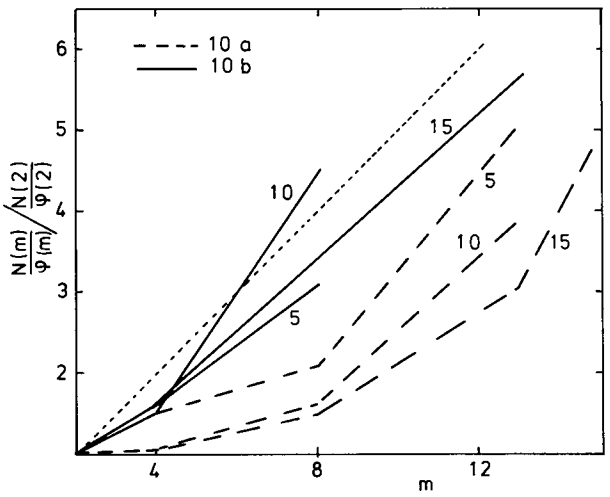

Fig. 4. $N_p(m)$ is the number of pairs with total mass m and separation smaller than the characteristic interparticle distance. The fraction of all pairs having total mass m is $\phi(m)$. The ratio of these quantities normalised to the value for $m=2$ is plotted at different times in models 10a and b. The time is in units of 10^9 yr. The dotted line is the prediction from Eq. (4)

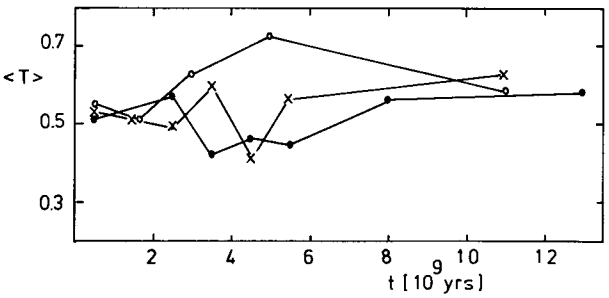

Fig. 5. Evolution of $\langle T\rangle$ [Eq. (5)] in model 10a (crosses), b (dots) and c (open circles). T was determined in a single run of each model

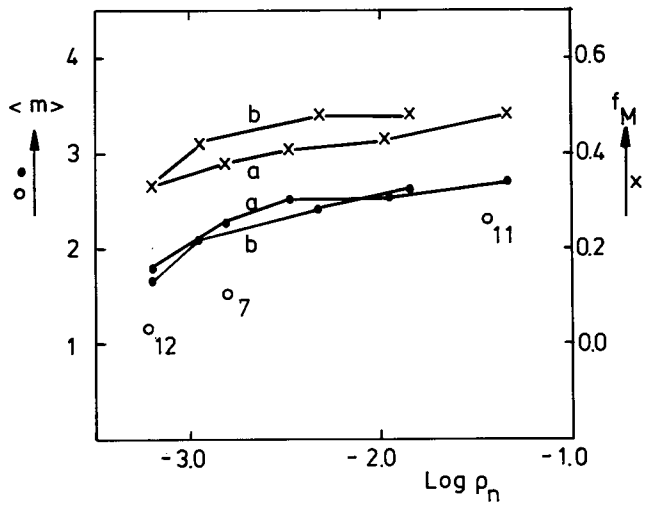

Fig. 6. Mean mass (filled circles) and fraction of merged galaxies (crosses) as a function of neighbour density around galaxies in model 10(a and b). Open circles give the over-all values of $\langle m\rangle$ in models 7, 11, and 12

interval and the average value of f_M and $\langle m\rangle_M$ respectively over this interval. For models 10a, b, and c we find results consistent with (6) at early epochs, but at late epochs N_{UU} is too small in models 10a and c probably due to depressed merging rates for smaller galaxies as described earlier (Fig. 4).

Equation (6) implies that on scales $\sim R_1$, the fraction of massive (or merged) particles is given by

$$f'_M=\tfrac{1}{2}[\langle m\rangle_M/\langle m\rangle+1]f_M, \tag{7}$$

where f_M is the overall fraction of merged galaxies and $\langle m\rangle$ is the mean mass per galaxy. Inside spheres of chosen radius S, centered on the galaxies, the mean fraction of merged galaxies, mean mass per galaxy and mean number density of galaxies, ϱ_m was calculated. The results for several values of S are plotted in Fig. 6. The open circles give the overall degree of merging measured by $\langle m\rangle=N_i/N_f$ as a function of average density in models 11 and 12 ($S=R_f$), while the filled circles give the degree of merging in model 10 as one goes to smaller scales corresponding to higher densities. On the smallest scales the fraction of merged galaxies is $\simeq 0.45$ in good agreement with (7) since $\langle m\rangle_M/\langle m\rangle\simeq 3.5/1.7\simeq 2$ and $f_M=0.3$.

The fraction of merged galaxies and the mean mass of galaxies increases slowly with increasing neighbour density. A crude linear fit to the experimental relation is

$$f_M\simeq 0.2\ \langle m\rangle\simeq 0.1\ \log\varrho_n+0.6. \tag{8}$$

To summarize, the simulations indicate the following clustering properties of merged galaxies.

(i) It is possible to model the merging probability of a pair of galaxies by assuming that it is proportional to the sum of the masses of the two merging galaxies. This dependence of the merging probability on mass implies that the covariance function of merged galaxies is amplified and slightly steepened on small scales.

(ii) The fraction of merged galaxies and the mean galaxy mass increase slowly with the neighbour density. On a local scale the merged galaxy fraction is well described by (7).

3.3. Mass Functions

In Fig. 7 some final mass-functions are given. The mass functions in models 10a, b, c are very similar and can be approximated by a simple powerlaw $n(m)dm\propto m^{\alpha}dm$ with $\alpha\simeq -2.2$ as also found by JE. This value of α is found to be independent of galaxy radius in contrast to the work of AF who find a slope of $\alpha\simeq -3$ for small galaxy radius. However, when the loss of orbital energy in non-merger collisions is zero we also obtain a steeper final mass function approaching $\alpha=-3$.

The final mass function in model 11 illustrates the effect of mass-loss. The mean mass of unmerged particles does not decrease significantly during a run with mass-loss included, since most collisions lead to mergers. The final fraction of the total mass in background particles is about 1/5 (or $\sim\frac{1}{2}\Delta N/N_i$) when $K\simeq 1$ and somewhat lower when $K\simeq 0.5$. As noted in Sect. 2.3, our prescription for mass-loss should be regarded as an upper limit.

The mass function evolution was simulated with a Monte Carlo code under the assumption that the merging probability is prescribed by (4). All galaxies had equal mass initially ($N_i=3000$). Results are given in Fig. 8. In model 10 we found $N_f/N_i\simeq 0.6$. The mass function obtained in the simulation when $N/N_i=0.6$ has slope $\alpha=-2.2$ in good agreement with the final mass function in 10. We conclude that the general evolution of the mass function can be explained by (4).

Table 2

Model	N_{UU}:	N_{UM} :	N_{MM}	t [10^9 yr]	f_M	$\langle m\rangle_M$
10a exp	1 :	0.64±0.14:	0.13±0.05	$1<t<3$	0.19	2.36
theor.	1 :	0.79 :	0.13			
10a exp.	1 :	3.5 ±0.8 :	0.9 ±0.3	$3<t<16$	0.29	3.02
theor.	1 :	1.65 :	0.51			
b exp	1 :	1.2 ±0.1 :	0.3 ±0.1	$3<t<16$	0.23	2.9
theor.	1 :	1.15 :	0.25			
c exp	1 :	2.4 ±0.4 :	0.5 ±0.2	$3<t<16$	0.20	2.92
theor.	1 :	0.98 :	0.19			

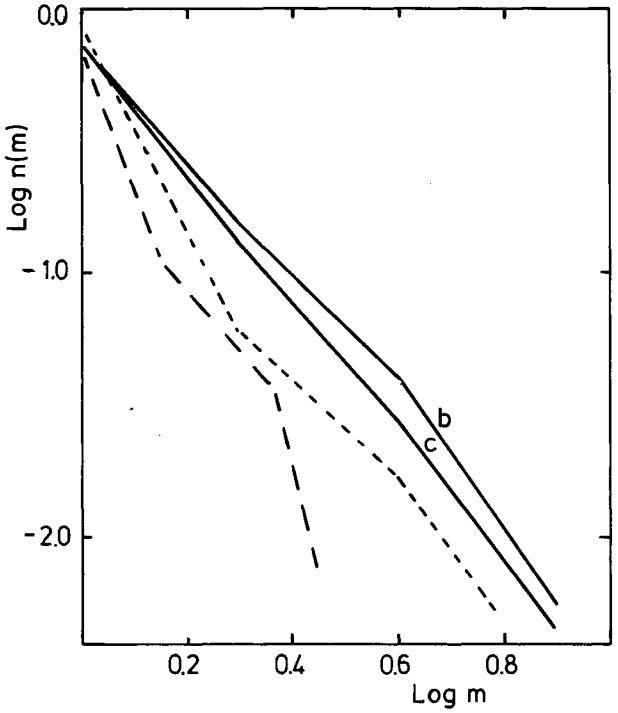

Fig. 7. Fraction of the total number of particles per unit interval of mass at t_f. Full lines are the results for model 10a and b. The dashed line is the final mass function in model 11, showing the effect of mass-loss. The dotted line shows the final mass function in model 10c when loss of energy in collisions not resulting in mergers is zero

When the simulations are continued the mass function reaches a self-similar form with $\alpha=-1.5$. This limiting form was also found in numerical experiments by Nakano (1966) and is in agreement with the self-similar solution of the coagulation equation when the cross-section of the particles is proportional to their mass (Trubnikov, 1971; Silk and White, 1978). Trubnikov's solution: $n(m)dm \propto m^{-1.5}e^{-m/m^*}dm$ is identical to the Press and Schechter (1971) mass function in the Poisson case. Therefore, Eq. (4) yields the proper limiting form of the mass function and we expect that the galaxy mass function evolves according to (4) as long as all galaxies in collapsed systems merge and no clusters form. It will describe the evolution of the cluster mass function or multiplicity function when merging ceases.

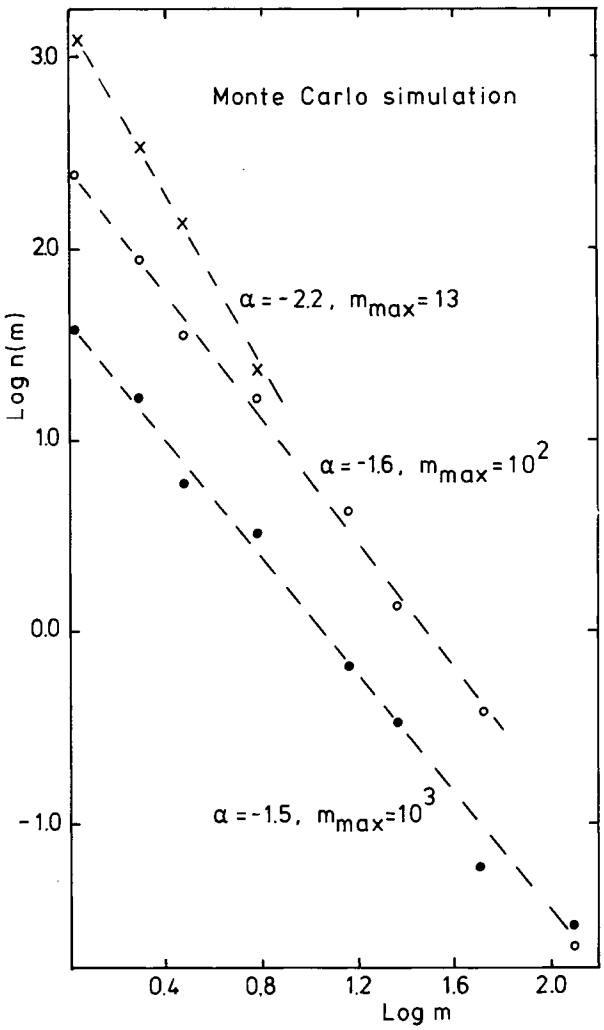

Fig. 8. Evolution of the mass function in the Monte Carlo simulation with 3000 equal mass particles initially. The dashed lines are powerlaw approximations to the mass functions for $N_i/N=1.6$ (crosses), 5.5 (open circles) and 33 (filled circles)

4. Comparison with Observations

The question we now turn to is whether one can identify systems that have undergone significant merging. The simulations give

Table 3

			G	$\bar{A}_{SS}$:	$\bar{A}_{SG}$:	$\bar{A}_{GG}$	k	λ
DG		Sample I	E	1	: 1.7 :	6.5	3.1	1.5
			S0	1	: 1.5 :	5.8	3.0	1.5
		Sample II	E	1	: 1.5 :	7.7	3.8	1.9
			S0	1	: 1.3 :	4.1	2.5	1.6
	f_G	f_S	G	N_{SS}:	N_{SG}:	N_{GG}		
KK	0.17	0.83	E+S0	1	: 0.48:	0.22	3.2	2.0
NI	0.10	0.55	E	1	: 0.5 :	0.16	3.5	2.5
NII	0.17	0.55	S0	1	: 0.47:	0.18	1.9	1.8

two clues from analysis of the fraction of merged galaxies and the clustering properties of merged galaxies. In fact we show that these properties support the hypothesis that elliptical and lenticular galaxies arise from merging spirals. We shall discuss later additional evidence from the intrinsic properties of early type galaxies in support of such a galaxy formation model.

4.1. The Fraction of Early Type Galaxies

The fraction of merged galaxies in the simulations is somewhat higher than the fraction of elliptical galaxies. However, the agreement is surprisingly good considering the uncertainties in our model and in the specific interpretation of the observations.

The observed fraction of elliptical galaxies among the bright galaxies in magnitude limited samples is about 0.1–0.15. The total fraction of elliptical and lenticular galaxies is about 0.2–0.3. These fractions depend on the luminosity function of galaxies of different types. There is observational evidence that the fraction of ellipticals among bright galaxies increases with luminosity, the mean absolute magnitude of ellipticals being brighter than spirals by about half a magnitude (Van den Bergh and McClure, 1979). This would make the real fraction of elliptical galaxies 0.05–0.08. The uncertainties in the simulations arise from: (i) the unrealistic initial mass function. (ii) the choice of the initial distribution of the particles, (iii) the merging process strongly inhibiting the formation of clusters in our simulations. This is most pronounced in model 10b although the galaxies in 10b have the realistic circular rotation velocity of ~ 250 km s^{-1}. It is possible that small visible cores of halos do not merge as easily as the halos they are embedded in. They might not merge at all when the galaxies are part of a collapsing cluster as in the White and Rees (1978) model.

4.2. Clustering Properties of Early Type Galaxies

We first note that the fraction of merged galaxies in the simulations is a very weak function of neighbour density (Fig. 4). Dressler (1979) has investigated the observed galaxy composition as a function of density in 55 clusters of galaxies. He finds that the fraction of E and SO galaxies varies slowly over a range of about three orders of magnitude in projected density. He also finds that at low densities the fraction of SO galaxies rises faster with density than the fraction of elliptical galaxies. In Sect. 5 we will see that these results fit naturally in the merger picture. The amount of clustering among galaxies in a magnitude limited survey depends on the depth of the catalogue, which is determined by the characteristic luminosity of the galaxies. The measured amount of clustering is sensitive to the bright end of the luminosity function (Peebles and Hauser, 1974). The luminosity functions of E, SO and spiral galaxies are very similar. However there is evidence that the average luminosity of ellipticals brighter than $M_v = -19$ is higher than disk galaxies by about a factor $\lambda \simeq 2$ (Van den Bergh and McClure, 1979). Therefore, in interpreting the observed correlation functions, we use the following crude rules: (1) The real clustering scales with the depth D of the catalogue as $A \propto D^{-\gamma} \propto \lambda^{-\gamma/2}$ or $A \propto \lambda$ if we use $\gamma = -2$, (2) The observations underestimate the cross-correlation between elliptical or SO and spiral galaxies by a factor $\lambda^{3/2}$ (or $\lambda^{-3/2}$ if $\lambda < 1$).

We first compare the simulation results with those of Davis and Geller (1976, DG) who study galaxy correlations as a function of morphological type. Specifically they use two samples (I and II) of galaxies from the Uppsala Catalogue to study the covariance functions of E, SO and spiral galaxies. Sample II is identical to sample I except that the galaxies in the Virgo and Coma clusters are excluded. Their results show that the correlation functions for E and SO galaxies are indeed higher and have a steeper slope as described in Sect. 3.2. The number of spiral neighbours within a distance r of an elliptical galaxy can be calculated from the amplitude A_{ES} and slope γ_{ES} of the cross correlation function for ellipticals and spirals by

$$n_{ES}(<r) = 4\pi \bar{n}_S A_{ES} (\gamma_{ES}+3)^{-1} r^{\gamma_{ES}+3}$$

where $\bar{n}_S$ is the mean number density of spiral galaxies. The number of galaxies on a local scale, say ~ 1 Mpc, is $n_{ES} = 4\pi \bar{n}_S \bar{A}_{ES}$, where $\bar{A}_{ES} = A_{ES}(\gamma_{ES}+3)^{-1}$. The relative numbers of close pairs of different types can be estimated from

$$N_{SS} : N_{ES} : N_{EE} = n_{SS} : n_{ES} \frac{\bar{n}_E}{\bar{n}_S} : n_{EE} \frac{\bar{n}_E}{\bar{n}_S} = \bar{A}_{SS} : 2 \frac{\bar{n}_E}{\bar{n}_S} \bar{A}_{ES} : \left(\frac{\bar{n}_E}{\bar{n}_S}\right)^2 A_{EE}.$$

In our simulations Eq. (6) was valid as long as virialised clusters did not form. Galaxies have formed virialised clusters and we will assume that during the collapse of these clusters (6) was valid and a fraction of ellipticals given by (7) was formed in high density regions. In these virialised regions galaxies meet randomly. Thus, we assume that

$$N_{SS} : N_{ES} : N_{EE} = 1 : 2 f_E'/f_S' : (f_E'/f_S')^2.$$

where

$$f_E'/f_S' = k f_E/f_S$$

and

$$k = \tfrac{1}{2}(\langle m \rangle_E / \langle m \rangle_S + 1). \tag{9}$$

Therefore

$$\bar{A}_{SS} : \bar{A}_{ES} : \bar{A}_{EE} = 1 : k : k^2.$$

Correcting for a difference in mean luminosity between E and S galaxies as discussed previously, we find for the observed ratios ($\lambda > 1$)

$$\bar{A}_{SS} : \bar{A}_{ES} : \bar{A}_{EE} = 1 : k/\lambda^{3/2} : k^2/\lambda. \tag{10}$$

In Table 3 the ratios for sample I and II of *DG* are given together with the values for k and λ derived from (10). The mass of E and SO galaxies derived in this way gives $\langle m \rangle_{E+SO} / \langle m \rangle_S \simeq 5$ which is slightly larger than the mass of merged galaxies in the simulations. The results in Table 3 further imply that E and SO galaxies have a larger mean brightness and a larger mass-to-light ratio than spiral galaxies.

We can also make a comparison with the work of Van Albada (1979) who has studied the small scale clustering of galaxies in the Uppsala Catalogue. The galaxies were divided into 10 intervals of 0.5 apparent magnitude. For each galaxy the 10 nearest neighbours were listed (in all 10 mag intervals separately). A local background density is estimated from the angular distance r to the 10th nearest neighbour which gives the expected value of the distance to the nearest neighbour, $\langle r_1 \rangle$, assuming a random distribution of galaxies. The observed distribution of $x = r/\langle r_1 \rangle$ can be compared with the Poisson distribution after normalisation of the two distributions for $x > 1$. In this way the excess of the galaxy density over the *local* density at $x < 1$ is found. For $x < 1$ and for an apparent magnitude difference between a galaxy and its neighbour less than 2.5 mag the excess densities P_E and P_{SO} of galaxies around E and SO galaxies are larger than around spiral galaxies. Van Albada's results yield

$$P_S : P_{SO} : P_E = 1 : 1.6 : 3.2$$

indicating that the clustering behaviour and hence probably also the mass of SO galaxies is intermediate between that of elliptical and spiral galaxies.

The fraction of ellipticals in groups with small crossing times (Field and Saslaw, 1971) is larger than the overall fraction. This also holds for galaxies in binaries. Karachentsev and Karachentseva (1974, KK) classify 17% of the galaxies in their catalogue as ellipticals (taking ellipticals and lenticulars together), while their sample of 1206 double galaxies contains 27% ellipticals. In Turner's sample of binaries (Turner, 1976a) there are 94 pairs containing only galaxies classified as pure E or pure S (Noerdlinger, 1979a, NI). The classification is taken from the Uppsala catalogue containing 10% ellipticals and 55% spirals. The subsample contains 21% ellipticals. Following the arguments leading to (10) the ratios of the numbers of SS, ES, and EE pairs are

$$N_{SS} : N_{SE} : N_{EE} = 1 : \frac{2k}{\lambda^{3/2}} f_E/f_S : \frac{k^2}{\lambda} (f_E/f_S)^2.$$

The observed ratios in the KK and NI sample and in a sample of binaries containing only SO galaxies (Noerdlinger, 1979b, NII) are given in Table 3. The second and third column contain the overall fraction of early-type and spiral galaxies. The values of k and λ derived from the observed ratios agree with those found from the covariance functions. We conclude that the covariance function data and the data on binaries are consistent with the interpretation of early-type galaxies as merger products.

Although the evidence presented here cannot be regarded as particular convincing proof, the data do suggest that the number of neighbours around a mass-concentration is indeed correlated with mass and luminosity. We shall pause briefly here to discuss some additional evidence.

As noted by GTA (1979) the forms of the observed 3- and 4-point correlation functions are consistent with the infall model. They also note that the observed ratio of the excess density of galaxies around Abell clusters over the excess density around galaxies (Seldner and Peebles, 1977) can be explained in this model.

Longair and Seldner (1979) have measured the cross-correlation function between the positions of 3 CR-radiogalaxies (R) having redshifts $z < 0.1$ and positions of the Lick galaxy counts (G). They find $A_{RG} = 4$ à 5 A_{GG}. This is expected if the number of neighbours on a local scale is proportional to mass, since strong radiosources have $\langle M_V \rangle = -2.3$ which is about 1.5 mag brighter than normal galaxies in a magnitude limited survey (Sandage, 1972a; Auriemma et al., 1977).

When binaries are formed according to (4) they will preferentially contain massive galaxies. We expect that their mass function has a higher characteristic mass and flatter slope than the field mass function. Recently White and Valdès (1980) have studied the luminosity function of close binary galaxies. They find that the luminosity function of these galaxies has a higher characteristic luminosity but does not show a flatter slope at the faint end relative to Felten's field luminosity function (1977) as would be expected. In another recent study Heiligman and Turner (1980) find that the luminosity function of galaxies in compact groups is flatter than the field luminosity function. It seems that both studies agree qualitatively that in binaries as well as in compact groups massive galaxies are overrepresented relative to the field.

5. Evolution of Galaxy Mass-functions and the Origin of Morphological Types

Let us now investigate the evolution of a more realistic mass function due to merging or infall during the epoch of cluster formation. We note here that not only ellipticals, but also bulges of disk galaxies might be formed by merging. Consider a small galaxy falling in a larger one. It will spiral towards its centre losing orbital energy and angular momentum through dynamical friction. The orbital energy will be transformed partly into internal energy of the disk. The disk will be heated but may survive if the infallen mass is smaller than the disk mass, and the bulge will grow. We then expect that galaxies with large bulge-to-disk ratio have stellar disks that are hotter than galaxies with low B/D. Recent observational studies, indicate that SO galaxies have bulge-to-disk ratios (B/D) which are systematically larger than those of spiral galaxies (Dressler, 1979; Burstein, 1979a). These galaxies appear to have "thick disks" as well (Tsikoudi, 1977; Burstein, 1979b). The colours and gas content of SO's indicate that they form a class intermediate between spirals and ellipticals. Their clustering properties, B/D-ratio and disk structure now suggest that they are the results of mergers between galaxies of unequal mass. We attempt to discuss this quantitatively in the following model.

5.1. The Model

Let us speculate that all bright ($M_V \lesssim -16$) galaxies were initially formed as disk galaxies resembling late-type spirals. It is proposed that these galaxies evolve along the sequence (Sc–Sb–Sa)–SO–E as they merge with other (smaller) galaxies in the subsequent clustering process. A key parameter determining the galaxy's morphological type in such a model will be Δ, the ratio of the accreted mass to the original mass.

We have chosen an initial mass function which simulates the observed galaxy luminosity function (Schechter, 1976)

$$\begin{aligned} n(m/m^*)\,d(m/m^*) &= (m/m^*)^{-1.25} && 0.015 < m/m^* < 1 \\ &= (m/m^*)^{-2.75} && 1 < m/m^* < 3 \\ &= 0 && m/m^* > 3 \end{aligned}$$

where $n(m)$ is the fraction of galaxies in the interval $(m/m^*, m/m^* + d(m/m^*))$ and m^* is the mass of a galaxy with absolute magnitude $M_V = -21.5$. The evolution of this mass function was numerically calculated using the Monte-Carlo code discussed in Sect. 3.3. Since the merging probability is proportional to the total mass of the merging galaxies, the most massive galaxies will swallow

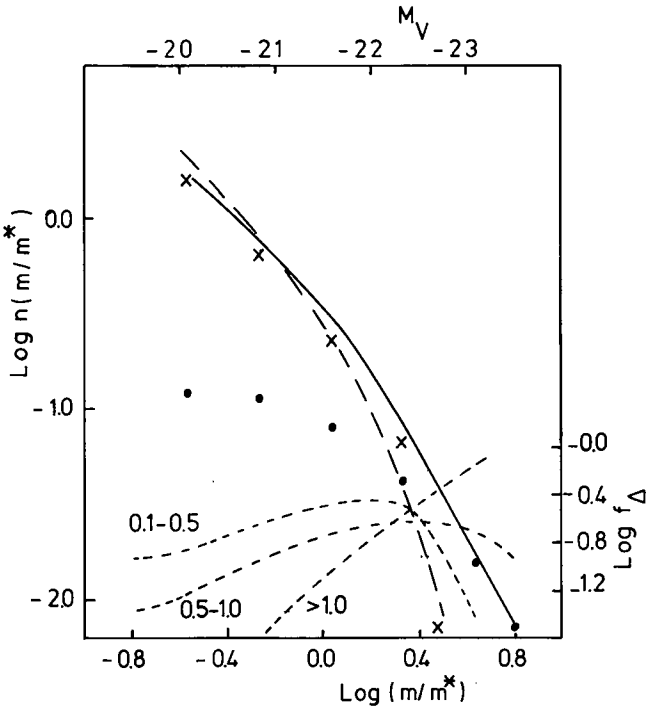

Fig. 9. Mass function for all particles (full line), for the particles with $\Delta < 0.5$ (crosses) and $\Delta > 0.5$ (dots) in the Monte Carlo simulation, when $\langle m\rangle/\langle m\rangle_i = 1.6$. The dashed line is the TYS luminosity function (see Sect. 5.3). The dotted lines give f_Δ, the fraction of galaxies having Δ within the range indicated near the curves

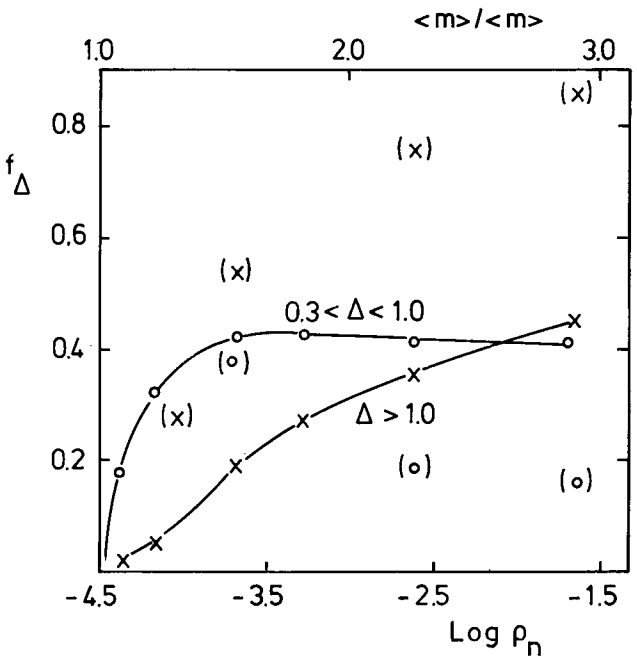

Fig. 10. Fraction of galaxies with $\Delta > 1$ (crosses) and $0.3 < \Delta < 1.0$ (open circles) plotted against $\langle m\rangle/\langle m\rangle_i$ and neighbourdensity ϱ_n. The fractions were calculated for $m > 0.4\ m^*$ (full lines) and for $m > m^*$ (between brackets)

Table 4

$\langle m\rangle/\langle m\rangle_i$ $[\langle m\rangle_i = 0.86\ m^*]$		$\Delta < 0.1$	$0.1 < \Delta < 0.5$	$0.5 < \Delta < 1.0$	$\Delta > 1.0$
1.1	f_Δ	0.81	0.11	0.06	0.02
	$\langle m\rangle_\Delta/m^*$	0.85	1.2	1.2	2.7
1.6	f_Δ	0.39	0.26 (0.18)	0.16 (0.20)	0.19 (0.54)
	$\langle m\rangle_\Delta/m^*$	0.75	1.13	1.2	2.9
2.0	f_Δ	0.28	0.24	0.18	0.3
	$\langle m\rangle_\Delta/m^*$	0.65	1.05	1.14	3.6

most mass. We shall study the mass function where the low-mass cut-off will have negligible effect, and we assume that at the present epoch $\langle m\rangle/\langle m\rangle_i \simeq 1.6$, as found in the N-body experiments. Here $\langle m\rangle_i$ is the mean initial mass for $m > 0.4\ m^*$.

5.2. *Results*

Results of the Monte Carlo simulations are given in Figs. 9 and 10 and in Table 4. Figure 9 gives the mass functions, when $\langle m\rangle/\langle m\rangle_i = 1.6$, for: (1) all galaxies, (2) galaxies having $\Delta > 0.5$, and (3) the galaxies having $\Delta < 0.5$. The mass-function for galaxies having $\Delta > 0.5$ is flatter than for other galaxies. In the same figure the fraction of galaxies f_Δ within a certain range of Δ, is plotted logarithmically against mass. Note that the slope of the mass function decreases with increasing Δ. Table 4 gives the fractions f_Δ and mean mass $\langle m\rangle_\Delta/m^*$ of the galaxies at three stages in the evolution of the mass function. All quantities were calculated for $m > 0.4\ m^*$. The fractions given in parentheses were calculated for $m > m^*$. It appears that f_Δ is quite sensitive to the choice of this lower limit. In Fig. 10 the relation between f_Δ and $\langle m\rangle_\Delta/\langle m\rangle_i$ is plotted for $0.3 < \Delta < 1.0$ and for $\Delta > 1.0$. We have used Eq. (8) to relate $\langle m\rangle/\langle m\rangle_i$ to the number density of galaxies ζ_n.

5.3. *Comparison with Observations*

Bulge-to-disk ratios are correlated with Hubble type (Roberts et al. 1975; Wakamatsu, 1976), but the range of bulge-to-disk masses that should be assigned to a Hubble type is uncertain.

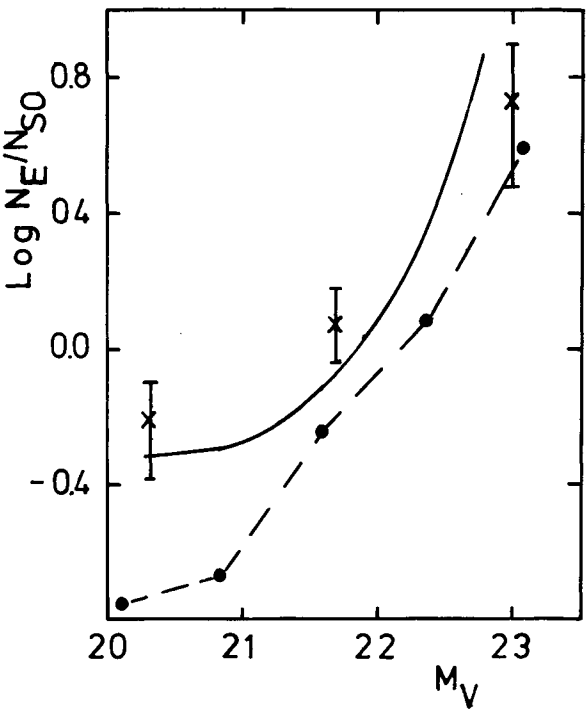

Fig. 11. Ratio of the number of ellipticals to the number of S0 galaxies from Van den Bergh and McClure (1979, crosses, the error bars are 1σ) and TYS (full line). The dashed line gives the result of the Monte Carlo simulation

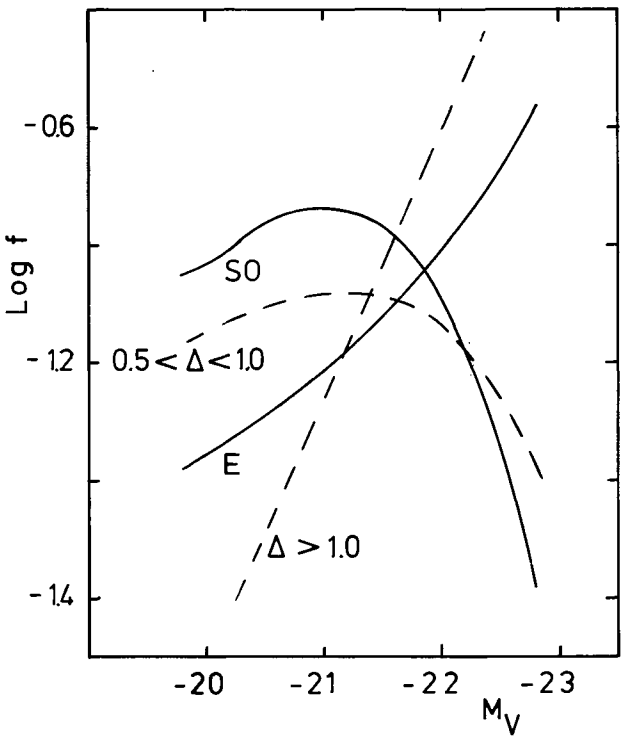

Fig. 12. The fraction of elliptical and S0 galaxies from TYS (full lines) and the results of the Monte Carlo simulation (dashed lines)

Burstein (1979a) has measured B/D values for three Sc and twelve SO galaxies. The B/D values of the spirals ranged from <0.07 to 0.2. Ten out of twelve SO galaxies had $0.5<B/D<1.5$. Quantitative estimates of B/D for different galaxy types are also given by Dressler (1979). These are 0.2, 0.2–0.5, and >0.5 for Sc, Sb, and Sa galaxies respectively. In regions of low galaxy density SO galaxies tend to have low B/D. There is typically a difference of about 1 mag between total and bulge magnitude for SO's in these regions suggesting that SO galaxies have $B/D\simeq 0.5$. The high B/D values for early type galaxies may partly be due to fading of the disk (Kent, 1980). Henceforth, we will assume that ellipticals have $\Delta>1.0$ and SO galaxies $0.5<\Delta<1.0$.

The mass function in Fig. 9 can be compared directly with luminosity functions of galaxies if M/L is taken to be constant (upper scale), the dots should be shifted to the left by $\simeq 0.75$ mag if $(M/L)_{E,SO}\simeq 2\,(M/L)_S$. The luminosity function for all galaxies (without correction for internal absorption) given by Tammann et al. (1979, TYS) normalised to our luminosity function is shown by the dashed line in Fig. 9. We have converted their magnitude scale to M_V using $M_V=M_B-0.8$. A shift in luminosity by ~ 0.75 mag for galaxies with $\Delta>0.5$ seems required to bring the functions in agreement. A more important result from Fig. 9 is that we expect the slope of the mass functions for different types to decrease with increasing B/D. We expect the fraction of ellipticals to increase almost linearly with mass.

Shapiro's (1971) data indicated that the luminosity function of ellipticals is indeed flatter than for other galaxies. The luminosity functions for spiral and SO galaxies presented by Dressler (1979) have a slope of about -2.5 for $M_V<-20.5$, while for ellipticals it is about -1.5. Van den Bergh and McClure (1979) have determined the luminosity function of E and SO galaxies from a sample studied by Sandage and Visvanathan (1978). The ratios of the number of E to the number of SO galaxies in this sample are given in Fig. 11. The ratios calculated from the TYS luminosity functions and the results of the Monte Carlo simulations are also shown. The slopes of the functions in the three cases are similar. Again, dimming of galaxies with $\Delta>0.5$ by about 0.75 mag would improve the fit.

In Fig. 12 the fractions of E and SO galaxies as a function of M_V from the TYS data are given. The dashed lines are the results from the Monte-Carlo simulation for $\Delta>1.0$ and $0.5<\Delta<1.0$. These fractions were calculated assuming $(M/L)_{\Delta<0.5}=2(M/L)_{\Delta<0.5}$. As expected a population of galaxies with small Δ has to be present before the population of galaxies with larger Δ can grow (Fig. 10). A similar behaviour for the frequencies of SO and E galaxies as a function of density was found by Dressler. His results apply to galaxies in rich clusters and are therefore not directly comparable to ours.

This preliminary exploration of a scenario in which bright galaxies are formed as late-type spirals which evolve along the sequence (Sc–Sa)–SO–E due to merging gives predictions that are already in qualitative agreement with observations in spite of all uncertainties discussed above.

6. Discussion

The general context in which we have placed the merging process in this paper is clearly different from the cannibalism process

described by Hausman and Ostriker (1978). If the galaxies are distributed at random initially, peaks in the density distribution, such as massive galaxies or proto-groups and clusters, will act as nuclei for the clustering process on local scales, the infall rates being proportional to mass. High-density peaks may exist in this initial distribution. Merging among the galaxies in these peaks may produce *cD*-galaxies which tend to gather clusters of galaxies around them afterwards via infall. In these clusters the massive galaxies lose orbital energy through dynamical friction and spiral towards the centre of the cluster where they can be cannibalised by a giant elliptical galaxy.

We have stressed in this paper how merging or infall might have played an important role in establishing the differences between the morphological types of galaxies. The model presented in Sect. 5 fits naturally in a scenario in which both galaxies and clusters form in a hierarchical clustering process such as the one discussed by White and Rees (1978). In their model, dark halos grow by gravitational clustering of objects formed shortly after recombination. Substructure is destroyed during the collapse of bound units. Any residual gas will, if ionised, be locked to the comoving frame by Compton drag on the microwave background. This would prevent it from falling into the potential wells of the halos until $z \simeq 50$ (Hogan, 1979). At some epoch ($z \gtrsim 10$) the gas will fall into the cores of the halos, cooling and forming rotating disks. The characteristic mass and radius of bright galaxies might have been determined by the criterium that cooling and collapse time-scales are comparable (Silk, 1977; Rees and Ostriker, 1977). Note that at low luminosities ($M_V \sim -18$) most galaxies are gas-rich spiral (Sc) and irregular galaxies. Below $M_V = -16$ we find only irregular galaxies and dwarf ellipticals. Many observed properties of galaxies such as the color-magnitude relation, constant central surface brightness and metallicity gradients may have been established during the epoch when dissipation played an important role (Tinsley and Larson, 1978; Norman and Silk, 1980). The observation that the present abundances of morphological types and the luminosity function of galaxies is at most weakly dependent on the density of the surrounding medium, however, suggests that the formation of predominantly stellar disk galaxies was completed before clusters of galaxies started to form. We have assumed that the presently observed bright galaxies descend from this population of galaxies. Clusters of galaxies will now be able to form since the relatively small luminous disks do not merge as easily as their halos. Nevertheless a considerable fraction of them will have merged with other galaxies by the present time. It seems plausible that this leads to the formation of a bulge, heating and even destruction of the stellar disks and depletion of its neutral gas content. These processes will occur preferentially at the high mass-end of the mass function and in regions of high galaxy density.

The product of a merger between two equal mass spiral galaxies is more massive but not necessarily more luminous if star formation ceases after the merging process is completed. Young stars in the arms of spiral galaxies contribute roughly 25% to the total light (in the *U*-band) of a spiral galaxy (Schweizer, 1976; Bash, F. private communication). This contribution disappears within $\sim 10^8$ yr. The subsequent decrease in luminosity is of order 0.5 mag in 10^{10} yr. (Sandage, 1972b; Tinsley, 1972). So after $\sim 10^{10}$ yr the luminosity of such a merged galaxy might be comparable to the luminosity of one spiral while its mass is twice as large. According to Turner (1976b) and to the results of this paper (Sects. 4.2 and 5) the mass-to-light ratio of ellipticals is indeed about twice as large as for spirals. Although no calculations of mergers of rotating stellar disks have been performed, there are indications that merger products of galaxies of comparable mass tend to have a Hubble density profile (White, 1979; Villumsen, 1979) and rotate slowly (JE, AF) as do elliptical galaxies. Recent observations indicate that bulges rotate faster than ellipticals (Illingworth et al., 1980; Kormendy and Illingworth, 1980). It will be interesting to see whether this is also consistent with the origin of bulges as proposed here. At the moment it seems that there is much evidence speaking in favor of a model in which merging is responsible of an evolution of bright galaxies along the sequence (Sc–Sb–Sa) –SO–E.

Conclusions

The numerical *N*-body simulations given here model the situation where clusteres of galaxies form from small random fluctuations in the initial distribution of galaxies corresponding to low initial velocity dispersion. The simulation particles, which all have equal mass initially are supposed to represent the halos of typical bright galaxies with $L = L^*$, and total mass-to-light ratio of about 150. The principal conclusions are as follows.

1. If the starting time of the simulations is chosen to produce about the observed amplitude of the covariance function, the final fraction of merged galaxies is typically 30%, varying from $\simeq 15\%$ in low density regions to $\simeq 50\%$ in high density regions. Since most mergers occur between glaxies in bound pairs, this fraction is very insensitive to galactic parameters and not particularly sensitive to either the final density or the final amplitude of the covariance function.

2. The galaxy collapse time estimated from the initial redshift in our simulations required to produce the observed amplitude of the covariance function is $\simeq 10^9$ yr for $\Omega \simeq 1$ and $\simeq 10^8$ yr for $\Omega = 1$.

3. The clustering properties and merging probability of the particles in the simulations are consistent with Eq. (4) as long as merging prevents the formation of clusters. When clusters form, the merging rate is depressed most strongly for the smallest particles.

4. The mass function is well described by a power-law approaching a self-similar form identical to the Press and Schechter mass function for an initially Poissonian distribution.

5. Observational data on the clustering properties of early-type galaxies are in good agreement with their interpretation as merged galaxies. Adopting this interpretation we find that the characteristic mass of ellipticals is several times larger than spirals while their luminosity is about a factor two larger. The clustering properties of SO galaxies suggest that their mass and luminosity is intermediate between that of spirals and ellipticals.

6. The form of the three and four-point correlation functions, the clustering of 3 C-radiogalaxies and the luminosity functions of galaxies in binaries and compact groups indicate that galaxy mass is indeed correlated with local galaxy density in our universe.

7. It is suggested that galaxies were formed as mainly stellar disks at $z \gtrsim 10$ and their luminous spherical components form by merging or infall during the subsequent epoch of cluster formation resulting in an evolution of galaxies along the sequence (Sc–Sb–Sa)–SO–E. This model predicts that the mass function of galaxies flattens from late to early-type galaxies. At the bright end of the luminosity function we expect to find mainly early-type galaxies. It is possible to explain qualitatively the observed frequencies of morphological types as a function of mass and neighbour density in this type of model.

Acknowledgements. I am very grateful to Sverre Aarseth for making his code available to me and for his friendly and helpful advise on how to incorporate collision effects. I wish to thank also Colin Norman for many useful discussions and thorough reading of the manuscript. Michael Fall and Simon White are acknowledged for many critical and useful comments on an earlier version of the manuscript. Tjeerd van Albada kindly provided his analysis of galaxy clustering prior to publication.

References

Aarseth, S.J., Gott, J.R., Turner, E.L.: 1979, *Astrophys. J.* **228**, 664
Aarseth, S.J., Fall, S.M.: 1979, *Astrophys. J.* **236**, 43
Auriemma, C., Perola, G.C., Ekers, R., Fanti, R., Lari, C., Jaffe, W., Ulrich, M.H.: 1977, *Astron. Astrophys.* **57**, 41
Burstein, D.: 1979a, *Astrophys. J.* **234**, 435
Burstein, D.: 1979b, *Astrophys. J.* **234**, 829
Chandrasekhar, S.: 1943, *Rev. Model. Phys.* **15**, 2
Davis, M., Geller, M.J.: 1976, *Astrophys. J.* **208**, 13
Dressler, A.: 1980, *Astrophys. J.* **236**, 351
Felten, J.E.: 1977, *Astron. J.* **82**, 861
Field, G.B., Saslaw, W.C.: 1971, *Astrophys. J.* **170**, 199
Gott, J.R., Rees, M.J.: 1975, *Astron. Astrophys.* **45**, 365
Gott, J.R., Turner, E.L.: 1976, *Astrophys. J.* **209**, 1
Gott, J.R., Turner, E.L., Aarseth, S.J.: 1980, *Astrophys. J.* **234**, 13
Gunn, J.E., Gott, J.R.: 1972, *Astrophys. J.* **176**, 1
Illingworth, G., Schechter, P.L., Gunn, J.E.: 1980 (in preparation)
Hausmann, M., Ostriker, J.P.: 1978, *Astrophys. J.* **224**, 320
Heiligman, G.M., Turner, E.L.: 1980, *Astrophys. J.* **236**, 745
Hogan, C.J.: 1979, *Monthly Notices Roy. Astron. Soc.* **188**, 781
Jones, B.J.T., Efstathiou, G.: 1979, *Monthly Notices Roy. Astron. Soc.* **189**, 27
Karachentsev, D., Karachentseva, V.E.: 1974, *Astron. Zh.* **51**, 724 (English transl. in *Soviet Astron. Astrophys. J.* **18**, 428
Kormendy, J., Illingworth, G.: 1980 (in preparation)
Longair, M.S., Seldner, M.: 1979, *Monthly Notices Roy. Astron. Soc.* **189**, 433
Miyoshi, K., Kihara, T.: 1975, *Publ. Astron. Soc. Japan* **27**, 333
Nakano, T.: 1966, *Progr. Theor. Phys.* **36**, 515
Noerdlinger, P.: 1979, *Astrophys. J.* **229**, 470
Noerdlinger, P.: 1979, *Astrophys. J.* **229**, 877
Peebles, P.J.B., Hauser, M.G.: 1974, *Astrophys. J. Suppl.* No. 253, **28**, 19
Press, W., Schechter, P.: 1974, *Astrophys. J.* **187**, 425
Rees, M.J., Ostriker, J.P.: 1977, *Monthly Notices Roy. Astron. Soc.* **179**, 541
Roberts, W.W., Roberts, M.S., Shu, F.H.: 1975, *Astrophys. J.* **196**, 381
Roos, N., Norman, C.A.: 1979, *Astron. Astrophys.* **76**, 75
Sandage, A.: 1972a, *Astrophys. J.* **178**, 1
Sandage, A.: 1972b, *Astrophys. J.* **178**, 25
Sandage, A., Visvanathan, N.: 1978, *Astrophys. J.* **228**, 742
Schechter, P.: 1976, *Astrophys. J.* **203**, 297
Seldner, M., Peebles, P.J.B.: 1977, *Astrophys. J.* **215**, 703
Shapiro, S.L.: 1971, *Astron. J.* **76**, 291
Silk, J.: 1977, *Astrophys. J.* **211**, 638
Silk, J., White, S.D.: 1978, *Astrophys. J.* **223**, L 59
Tammann, G.A., Yahil, A., Sandage, A.: 1979, *Astrophys. J.* **234**, 775
Tinsley, B.M.: 1972, *Astrophys. J.* **178**, 319
Tinsley, B.M., Larson, R.B.: 1979, *Monthly Notices Roy. Astron. Soc.* **186**, 503
Toomre, A., Toomre, J.: 1972, *Astrophys. J.* **178**, 662
Toomre, A.: 1977, in *The Evolution of Galaxies and Stellar Populations*, eds. B. M. Tinsley and R. B. Larson, New Haven: Yale University Observatory, p. 401
Trubnikov, B.A.: 1971, *Soviet. Phys. Doklay* **16**, 124
Tsikoudi, V.: 1979, *Astrophys. J.* **234**, 842
Turner, E.L.: 1976a, *Astrophys. J.* **208**, 20
Turner, E.L.: 1976b, *Astrophys. J.* **208**, 304
Turner, E.L., Gott, J.R.: 1976, *Astrophys. J.* **209**, 6
Turner, E.L., Aarseth, S.J., Gott, J.R., Blanchard, N.T., Matthieu, R.: 1979, *Astrophys. J.* **228**, 684
Van Albada, T.S.: 1980 (in preparation)
Van Albada, T.S., Van Gorkom, J.N.: 1977, *Astron. Astrophys.* **54**, 121
Van den Berg, S., McClure, R.D.: 1979, *Astrophys. J.* **231**, 671
Villumsen, J.V.: 1979 (preprint)
Wakamatsu, K.: 1976, *Publ. Astron. Soc. Japan* **28**, 397
White, S.D.M., Rees, M.J.: 1978, *Monthly Notices Roy. Astron. Soc.* **183**, 341
White, S.D.M.: 1978, *Monthly Notices Roy. Astron. Soc.* **184**, 185
White, S.D.M.: 1979, *Monthly Notices Roy. Astron. Soc.* **189**, 831
White, S.D.M., Valdès, F.: 1980, *Monthly Notices Roy. Astron. Soc.* **190**, 55